JMEPEG (2012) 21:1714–1723
DOI: 10.1007/s11665-011-0088-9

1059-9495/$19.00

Kinetics and Boron Diffusion in the FeB/Fe_2B Layers Formed at the Surface of Borided High-Alloy Steel

I. Campos-Silva, M. Ortiz-Domínguez, C. Tapia-Quintero, G. Rodríguez-Castro, M.Y. Jiménez-Reyes, and E. Chávez-Gutiérrez

(Submitted October 29, 2010; in revised form June 19, 2011)

In the present study, boron diffusion in the surface layers of AISI M2 borided steels and the growth kinetics of the FeB/Fe_2B layers were estimated. The boriding of AISI M2 steel was performed according to the powder-pack method and was conducted at 1173-1323 K and at various exposure times. As a result of the boriding process, the diffusion-controlled growth of the FeB/Fe_2B layers was obtained at the surface of the high-alloy steel, and the kinetics of the growth process changed parabolically over time. The boron diffusion coefficients were estimated by solving two simultaneous equations based on the limits of the boron concentration in each layer, the boride incubation time, and the parabolic growth constant. With the proposed diffusion model, an expression, which describes the evolution of the FeB/Fe_2B layers, was obtained. Moreover, the proposed model and diverse empirical models presented in the literature provided a good fit to the experimental data obtained for 10 h of exposure and different boriding temperatures.

Keywords boride layers, boriding, boron diffusion coefficients, diffusion model, growth kinetics

1. Introduction

Boriding is a thermochemical surface treatment, whereby boron is diffused into, and combines with, the substrate material forming a single- or double-phase metal boride layer at the surface. Unlike many other surface treatments, hard boride layers can be developed on most alloys and metals by boron diffusion. The boriding of ferrous materials results in the formation of either a single layer (Fe_2B) or double-layer (FeB/Fe_2B) with definite composition. The thickness of the layer formed (known as the case depth), which affects the mechanical and chemical behavior of borided steels, depends on the boriding temperature, the treatment time, and the boron potential that surrounds the surface sample (Ref 1). The optimum boride layer thickness for low-carbon steels and low-alloy steels ranges from 50 to 250 μm, while the optimum boride layer thickness for high-alloy steels ranges from 25 to 76 μm (Ref 2). In addition, the thickness of the boride layer has an effect on the dimensions and superficial roughness of the materials exposed to the treatment. It has been demonstrated that the dimensions of the borided samples increased by one-fifth to one-third of the total depth of boride coating (Ref 3). Therefore, the estimation of the kinetic parameters for the evolution of the FeB and Fe_2B surface layers during the boriding process is of great importance.

I. Campos-Silva, M. Ortiz-Domínguez, C. Tapia-Quintero, G. Rodríguez-Castro, M.Y. Jiménez-Reyes and **E. Chávez-Gutiérrez,** Instituto Politécnico Nacional, Grupo Ingeniería de Superficies, SEPI-ESIME, U.P. Adolfo López Mateos, Zacatenco, 07738 Mexico, D.F., Mexico. Contact e-mail: icampos@ipn.mx.

Interest in the study of the growth kinetics of boride layers in ferrous alloys has increased over the last 20 years (Ref 1, 4-14). Traditional diffusion models (Ref 4-6, 8) suggest that the FeB and Fe_2B layers obey the parabolic growth law $x^2 = Kt$, where x is the mean thickness of the boride layer, K is the growth constant, and t is the exposure time of the substrate to the boriding process. To estimate the activation energy (Q), the behavior of the growth constant as a function of the boriding temperature must be determined. Moreover, an accurate estimation of the activation energy is necessary to stimulate the formation of the boride layer at the steel surface. Other diffusion models based on the mass balance equations of the FeB/Fe_2B and the Fe_2B/substrate interface as well as the boron concentration profile of the surface layers have been developed (Ref 1, 5, 7, 9, 11-14). One solution to the mass balance equations of the surface layers is based on the parabolic growth law and can be used to estimate the boron diffusion coefficients of the FeB and Fe_2B layers (D_{FeB} and D_{Fe_2B}, respectively). The boron diffusion values obtained for each surface layer are represented by the Arrhenius equation; thus, the activation energy of the system must be known. Likewise, in many diffusion models, the boride incubation time (t_0) is considered to be an additional variable in the parabolic growth equation for the solution of the mass balance equation. The results of previous studies (Ref 14-16) have shown that the boride incubation time is dependent on the boriding temperature and decreases with an increase in temperature. Based on the experimental data of the boriding process, which includes exposure time, boride incubation time, temperature, and boron potential of the medium, several kinetic parameters have been estimated, including the weight gain due to the formation of boride layers at the surface of steel, the instantaneous velocity of the Fe_2B/substrate interface, and the boron diffusion coefficient of the Fe_2B layer, which is dependent on the parabolic growth constant and the $\left(\frac{t}{t_0}\right)$ ratio.

In the present study, a diffusion model was proposed to determine the boron diffusion coefficients of the FeB and Fe_2B layers at the surface of AISI M2 steel produced by powder-pack boriding. The diffusion model was based on the boron concen-

tration profiles of the surface layers, the parabolic growth law which considers the boride incubation time, and the mass balance equations of the FeB/Fe_2B and Fe_2B/substrate interfaces. The model was extended to evaluate variations in the thicknesses of the FeB/Fe_2B layers, and the results were compared to those of empirical models proposed in the literature.

2. Diffusion Model

A linear boron concentration profile was assumed for each of the boride layers formed at the steel surface. C^i_{up} and C^i_{low} represent the maximum and minimum boron concentration in the FeB and Fe_2B layers (i = FeB or Fe_2B), as shown in the Fe-B phase diagram (see Fig. 1a, b). The boride layers possessed a narrow range of boron concentrations of about 1 wt.% (Ref 17, 18). Likewise, the homogeneity of the distribution of boron in the FeB and Fe_2B layers can be described by a_1 and a_3, and the parameters a_2 and a_4 express the miscibility gap between the FeB/Fe_2B and Fe_2B/substrate layers, respectively. Finally, C_0 is the boron concentration in the γ-Fe phase (0.003 wt.% B).

The initial and boundary conditions of the diffusion problem were represented by the following equations, as shown in Fig. 1(c):

$$C_{FeB}[x(t=0)] = C_0; \quad C_{Fe_2B}[x(t=0)] = C_0; \tag{Eq 1}$$

$$C_{FeB}[x(t)] = C^{FeB}_{up} + \frac{C^{FeB}_{low} - C^{FeB}_{up}}{u}x(t) \tag{Eq 9}$$

$$C_{Fe_2B}[x(t)] = C^{Fe_2B}_{up} + \frac{C^{Fe_2B}_{low} - C^{Fe_2B}_{up}}{l}[x(t) - u] \tag{Eq 10}$$

If the substrate becomes saturated within a short period of time and the solubility of boron is extremely low in γ-Fe (0.003 wt.% B), then $J_3 = 0$. Thus, the fluxes J_1 and J_2 can be expressed by the following equations:

$$J_1 = D_{FeB}a_1/u \tag{Eq 11}$$

$$J_2 = D_{Fe_2B}a_3/l \tag{Eq 12}$$

where D_{FeB} is the boron diffusion coefficient of the FeB layer, D_{Fe_2B} is the boron diffusion coefficient of the Fe_2B layer, and u and l represent the depths of the FeB and Fe_2B layers, respectively.

By substituting Eq 11 and 12 into Eq 7 and 8, the mass balance equations of the interfaces can be expressed as

$$(a_2 + a_1/2)\frac{du}{dt} = D_{FeB}\frac{a_1}{u} - D_{Fe_2B}\frac{a_3}{l} \tag{Eq 13}$$

$$(a_4 + a_3)\frac{du}{dt} + (a_4 + a_3/2)\frac{dl}{dt} = D_{Fe_2B}\frac{a_3}{l} \tag{Eq 14}$$

Furthermore, the continuity Eq 13 and 14 can be rewritten as follows:

$$\left.\begin{aligned}
&C_{FeB}\left\{x\left[t = t_0^{FeB}(T)\right] = 0\right\} = C^{FeB}_{up} \quad \text{for } C^B_{ads} > 16.23\ \text{wt.\% B},\\
&C_{FeB}\left\{x\left[t = t_0^{FeB}(T)\right] = 0\right\} = C^{FeB}_{low} \quad \text{for } C^B_{ads} < 16.23\ \text{wt.\% B and with FeB layer},\\
&C_{Fe_2B}\left\{x\left[t = t_0^{Fe_2B}(T)\right] = 0\right\} = C^{Fe_2B}_{up} \quad \text{for } 8.83\ \text{wt.\% B} < C^B_{ads} < 16.23\ \text{wt.\% B and without FeB layer},\\
&C_{Fe_2B}\left\{x\left[t = t_0^{Fe_2B}(T)\right] = 0\right\} = C^{Fe_2B}_{low} \quad \text{for } C^B_{ads} < 8.83\ \text{wt.\% B and without FeB layer},
\end{aligned}\right\} \tag{Eq 2}$$

$$C_{FeB}[x(t=t) = u] = C^{FeB}_{low}, \tag{Eq 3}$$

$$C_{Fe_2B}[x(t=t) = u] = C^{Fe_2B}_{up}, \tag{Eq 4}$$

$$C_{Fe_2B}[x(t=t) = v] = C^{Fe_2B}_{low}, \tag{Eq 5}$$

$$C_{Fe_2B}[x(t=t) = v] = C_0, \tag{Eq 6}$$

C^B_{ads} represents the effective adsorbed boron concentration during the boriding process (Ref 9).

The mass balance equations of the FeB/Fe_2B and Fe_2B/substrate interfaces can be described as follows:

$$\Delta_{FeB} = a_2 du + \frac{1}{2}a_1 du = J_1 dt - J_2 dt \tag{Eq 7}$$

$$\Delta_{Fe_2B} = a_4(du + dl) + a_3 du + \frac{1}{2}a_3 dl = J_2 dt - J_3 dt \tag{Eq 8}$$

where J_1, J_2 and J_3 were obtained from Fick's First Law, $J = -D\{dC[x(t)]/dx(t)\}$. The equations that represent the boron concentration in the FeB and Fe_2B layers can be described as follows (see Fig. 1c):

$$\frac{du}{dt} = D_{FeB}P_1\frac{1}{u} - D_{Fe_2B}P_2\frac{1}{l} \tag{Eq 15}$$

$$\frac{dl}{dt} = D_{Fe_2B}P_3\frac{1}{l} - D_{FeB}P_4\frac{1}{u} \tag{Eq 16}$$

with $P_1 = \frac{a_1}{a_2 + a_1/2}$, $P_2 = \frac{a_3}{a_2 + a_1/2}$, $P_3 = a_3\frac{a_3 + a_4}{a_4 + a_3/2}\left(\frac{1}{a_3 + a_4} + \frac{1}{a_2 + a_1/2}\right)$, and $P_4 = \frac{a_3 + a_4}{a_4 + a_3/2}\left(\frac{a_1}{a_2 + a_1/2}\right)$

The solutions to Eq 15 and 16 can be obtained by considering the parabolic growth equations of the surface layers (Ref 1, 19, 20):

$$u = k_{FeB}\left(t - t_0^{FeB}(T)\right)^{1/2} \tag{Eq 17}$$

where k_{FeB} is the growth constant of the FeB layer, $t_0^{FeB}(T)$ is the boride incubation time as a function of the temperature, and $\left(t - t_0^{FeB}(T)\right)^{1/2}$ is the effective growth time of the FeB layer. In a similar manner, the growth equation of the Fe_2B layer can be defined as

$$l = v - u = k(t - t_0(T))^{1/2} - k_{FeB}\left(t - t_0^{FeB}(T)\right)^{1/2} \tag{Eq 18}$$

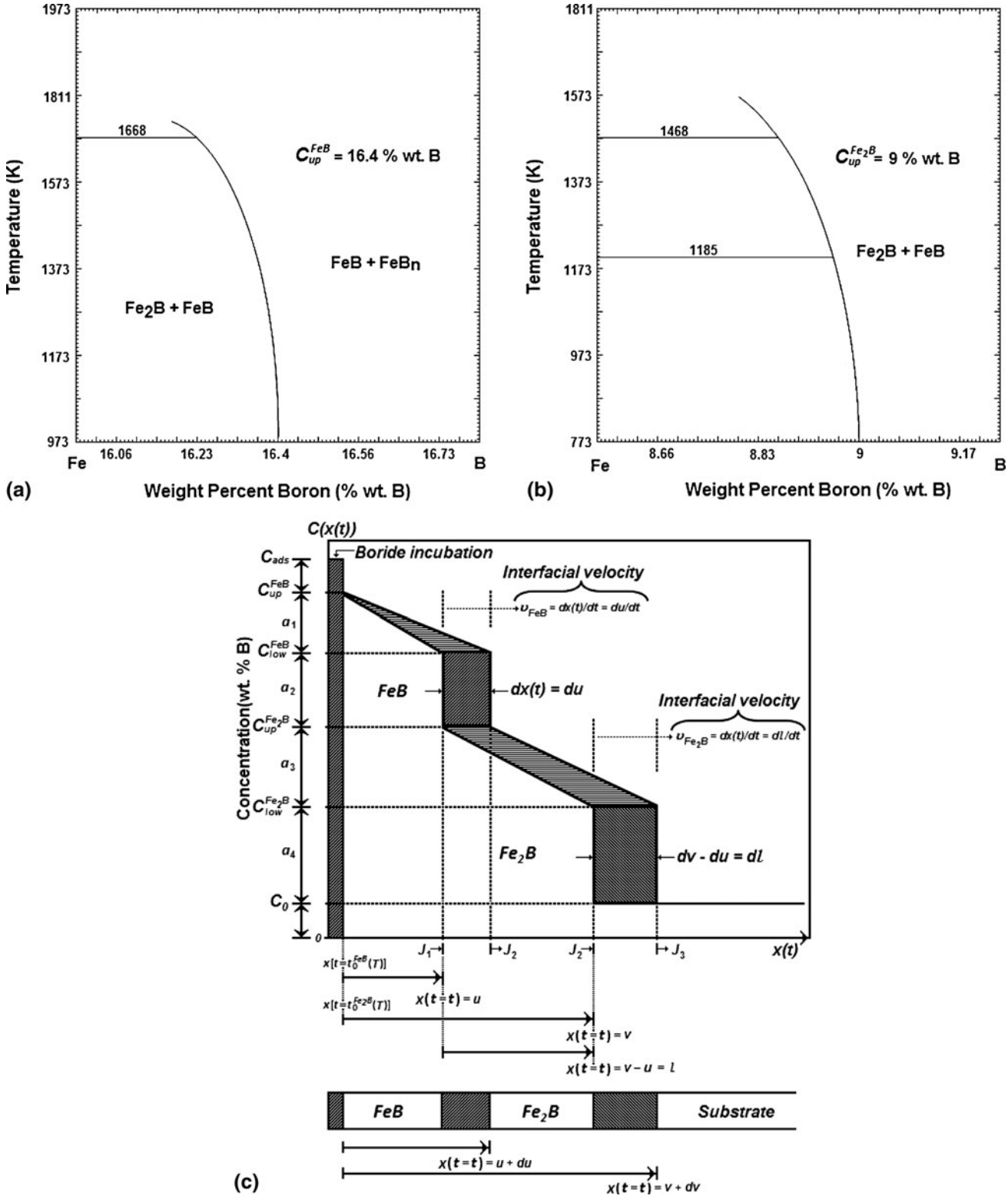

Fig. 1 (a) Schematic representation of the C_{up}^{FeB} and C_{low}^{FeB} values obtained from the Fe-B phase diagram for a range of temperatures, (b) schematic representation of the $C_{up}^{Fe_2B}$ and $C_{low}^{Fe_2B}$ values obtained from the Fe-B phase diagram for a range of temperatures, and (c) boron concentration profile in the FeB/Fe_2B layers

where v is the thickness of the total boride layer, t is the treatment time, $t_0(T)$ is the boride incubation time of the total boride layer ($t_0^{FeB}(T) > t_0(T)$), and k is the parabolic growth constant of the total boride layer.

Based on the aforementioned assumptions, the boron diffusion coefficients in the FeB and Fe_2B layers (D_{Fe_2B} and D_{FeB}) can be derived by applying Eq 15 and 16 as follows:

$$D_{Fe_2B} = \frac{l}{a_3}\left[(a_4 + a_3/2)\left(\frac{du}{dt} + \frac{dl}{dt}\right) + (a_3/2)\left(\frac{du}{dt}\right)\right], \quad m^2\,s^{-1} \tag{Eq 19}$$

$$D_{FeB} = \frac{u}{a_1}\left[(a_4 + a_3/2)\left(\frac{du}{dt} + \frac{dl}{dt}\right) + (a_3/2 + a_2 + a_1/2)\left(\frac{du}{dt}\right)\right], \quad m^2\,s^{-1} \tag{Eq 20}$$

3. Experimental Procedure

AISI M2 steels with a nominal composition of 0.85 wt.% C, 0.3 wt.% Mn, 0.3 wt.% Si, 4.5 wt.% Cr, 5 wt.% Mo, 1.95 wt.% V, and 6.40 wt.% W were sectioned into cubic samples with dimensions of 13 × 13 × 13 mm. The samples were embedded in a closed, cylindrical case (AISI 304L) containing a B_4C Durborid fresh powder mixture with a powder size of 50 μm. Both FeB and Fe_2B layers on the surface of the steel were grown at 1173, 1223, 1273, and 1323 K for 4, 6, and 8 h. Boriding was accomplished by placing the container in a furnace in the absence of inert gases, and the boriding time began when the temperature of the furnace reached the boriding temperature. When the treatment was complete, the container was removed from the furnace and was slowly cooled to room temperature.

Cross sections of the samples were prepared for microscopic examinations by standard metallographic techniques using GX51 Olympus equipment. Eighty measurements were performed from a fixed reference on different sections of borided samples to determine the FeB and the total layer thickness. In addition, x-ray diffraction (XRD) and energy dispersive x-ray spectroscopy (EDS) were conducted on material borided at 1223 K for 8 h to characterize the nature of the borided products and the distribution of heavy elements in the surface layers. For these purposes, a Siemens D5000 (Cu Kα radiation at λ = 1.54 A) diffractometer and a Leica Cambridge Stereoscan 440 spectrometer were employed. Finally, Vickers microindentation was conducted to evaluate the hardness-depth profile of the boride layers on the borided steel surface, and a constant indentation load of 50 g was applied to the samples by means of a Wolpert 402MVD apparatus.

4. Results and Discussions

The characteristics of borided AISI M2 steel indicated that the formation of FeB/Fe_2B layers was controlled by the diffusion of boron at the steel surface. Figure 2 shows the smooth morphology of the microstructure of the FeB/Fe_2B layers. The diffusion of boron was dependent on the crystallographic direction of anisotropic crystals in the boride layers. Nuclei of iron borides were oriented with respect to the surface in such a way that the crystallographic directions and lattice imperfections were oriented perpendicularly to the diffusion front, which caused the FeB/Fe_2B layers to grow in the direction of the substrate. Moreover, the growth rate and phase composition of the layers were determined by the activity of boron on the steel surface, the temperature of the boriding process, and the composition of the substrate. Once compact boride layers have formed on the surface, their growth can be described by the following reactions (Ref 21):

$$B_{dif} + Fe_2B = 2FeB \tag{Eq 21}$$

$$Fe_{dif} + FeB = Fe_2B \tag{Eq 22}$$

The presence of alloying elements in the steel reduces the growth rate of the boride layers because of the formation of a diffusion barrier, which slows the growth of the FeB/Fe_2B layer (Ref 22). In addition, the results of x-ray diffraction analysis, which are depicted in Fig. 3, revealed the presence of the iron borides at the steel surface. In addition, chromium and vanadium tend to dissolve in FeB/Fe_2B layers and form independent borides with a lattice constant similar to that of iron borides. Moreover, the results of previous studies suggest that chromium accumulates in the outermost region of the FeB/Fe_2B layer (see (Ref 23) and references therein). Alternatively, molybdenum displays a much lower tendency to dissolve in the boride layer and tends to concentrate beneath the surface layers (Ref 24). As shown in Fig. 4, the results of EDS analyses

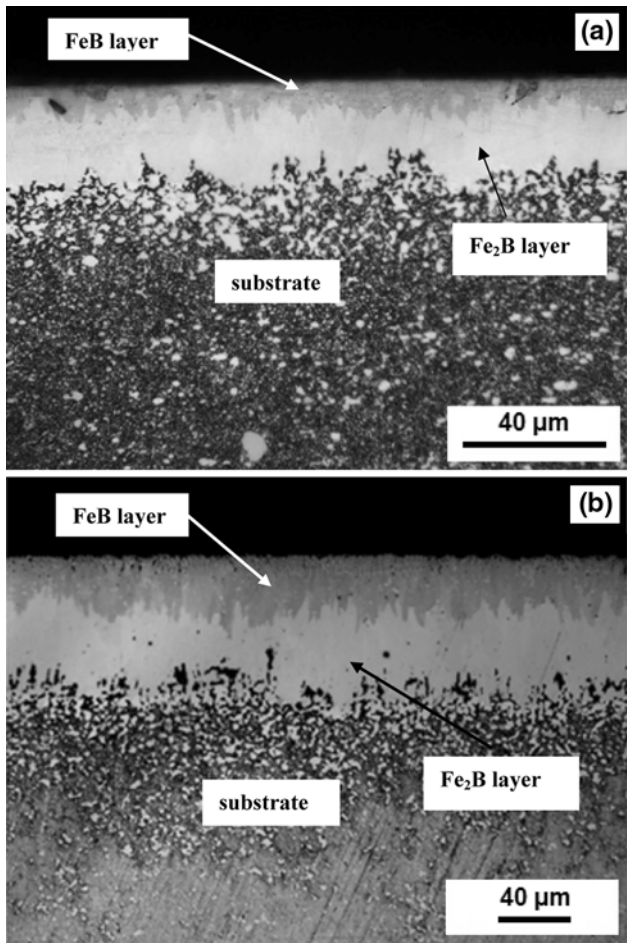

Fig. 2 Cross-sectional views of FeB and Fe_2B layers formed at the surface of AISI M2 steel with boriding conditions of (a) 1173 K with exposure time of 8 h, and (b) 1323 K with exposure time of 6 h

revealed that the chemical composition of the steel propitiates the dissolution of tungsten in the surface layer, which results in the formation of WC interstitial compounds.

Vickers microhardness indentations were applied along the FeB/Fe_2B layers of the samples produced at different boriding temperatures and exposure times, as shown in Fig. 5. At a distance of approximately 10 μm from the AISI M2 borided steel, the hardness values of the specimens approximately ranged from 1900 to 2700 HV. Moreover, at an exposure time of 8 h, the hardness of the boride layer decreased as the temperature increased to 1273 K, as shown in Fig. 6. As stated by Genel et al. (Ref 25), a reduction in the hardness of the layer can be attributed to grain coarsening. In contrast, according to Galibois et al. (Ref 26), thermal residual stresses produced by the growth of the surface layers and the difference between the specific volume of the substrate and the coating can have a significant effect on the hardness-depth profile.

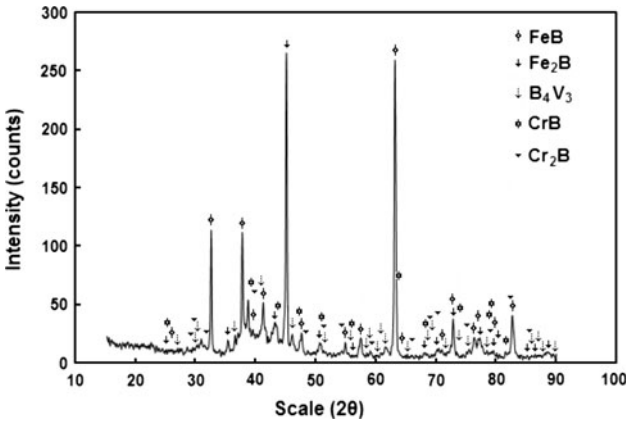

Fig. 3 XRD pattern of AISI M2 steel boriding at the temperature of 1273 K with 8 h of exposure

As shown in Fig. 7, the dependence of the thicknesses of the FeB layer (u) and the entire boride layer (FeB + Fe_2B) (v) on the exposure time was parabolic, which is indicative of diffusion-controlled growth. Moreover, for both layers, the boride incubation time decreased with an increase in boriding temperature. The values of k and k_{FeB} were obtained from the slope of the straight line shown in Fig. 7, and the boron diffusion coefficients of the Fe_2B and FeB layers, (D_{Fe_2B} and D_{FeB}, respectively) were obtained from Eq 19 and 20. The diffusion coefficients of each exposure time and boriding temperature were strongly related to the thickness of the boride

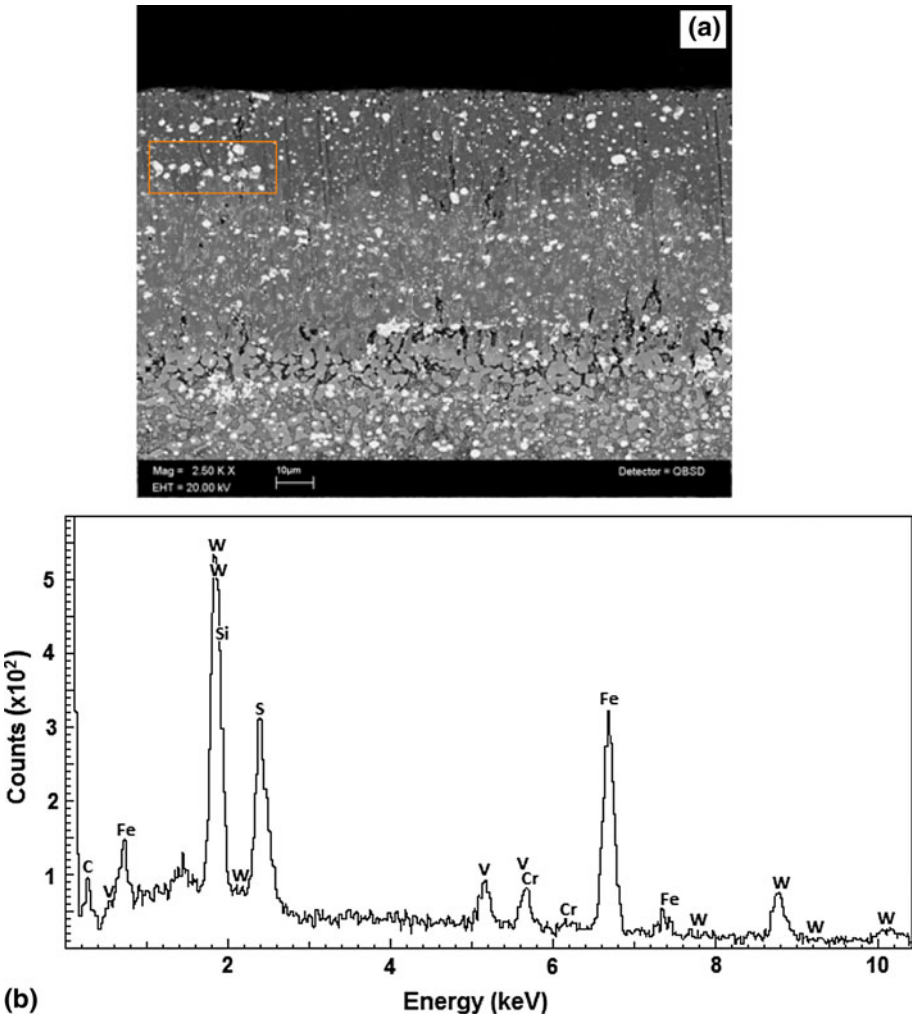

Fig. 4 (a) SEM image of cross-sectional view of AISI M2 steel boriding at 1273 K with 8 h of exposure and (b) EDS spectrum of the borided sample

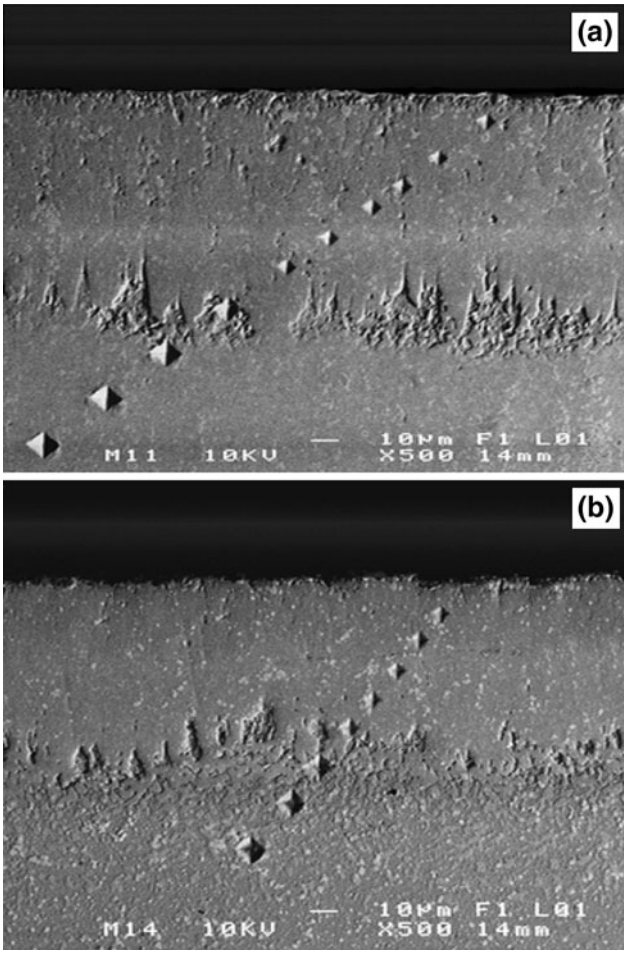

Fig. 5 Vickers microhardness testing performed across the FeB/Fe_2B layers formed in AISI M2 steel boriding at (a) 1273 K with 8 h of exposure and (b) 1323 K with 6 h of exposure

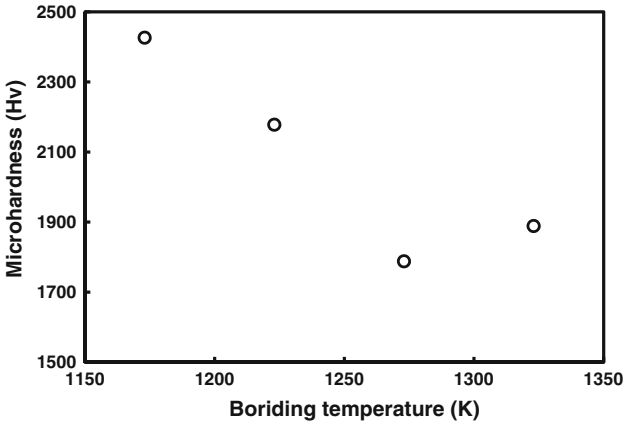

Fig. 6 Hardness behavior as a function of the boriding temperatures with 8 h of exposure at 10 µm from the surface of AISI M2 borided steel

layer. In the Arrhenius equation, the mean values of the diffusion coefficients were expressed as a function of the temperature, as shown in Fig. 8. The behaviors of the boron diffusion coefficients in the studied range of the boriding temperatures can be described by the following equations:

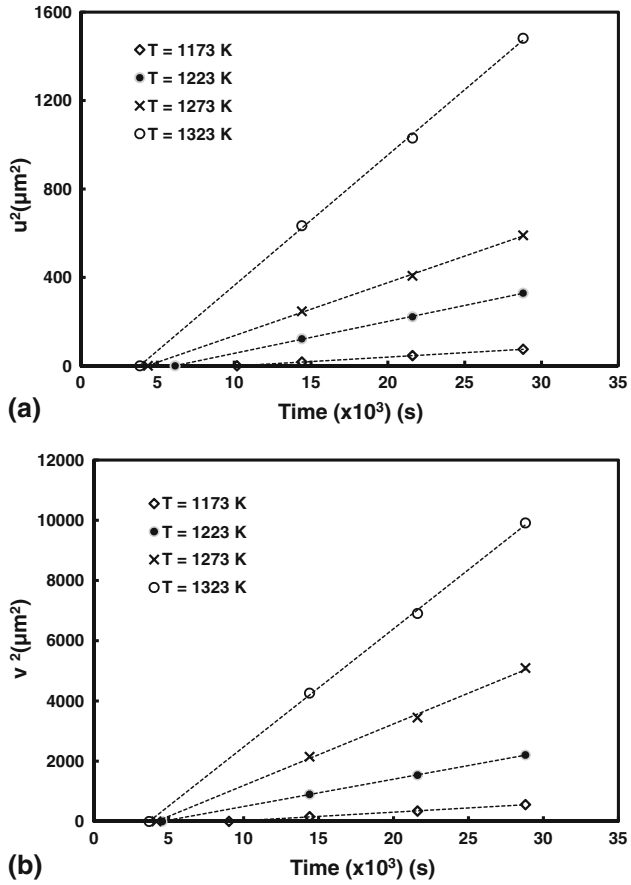

Fig. 7 (a) Evolution of the FeB layer as a function of exposure time and (b) Evolution of the (FeB + Fe_2B) layers as a function of exposure time

$$D_{Fe_2B} = 1.06 \times 10^{-3} \exp\left(-\frac{207\,\text{kJ/mol}}{RT}\right), \quad \text{m}^2\,\text{s}^{-1} \qquad \text{(Eq 23)}$$

$$D_{FeB} = 3.4 \times 10^{-3} \exp\left(-\frac{223\,\text{kJ/mol}}{RT}\right), \quad \text{m}^2\,\text{s}^{-1} \qquad \text{(Eq 24)}$$

The activation energies of both layers over the entire temperature range were indicative of homogeneous diffusion, and the pre-exponential factors were strongly dependent on the composition of the borided steel (Ref 22). The relatively high-activation energies shown in Table 1 were attributed to the formation of FeB, Fe_2B, CrB, and/or Cr_2B phases in the boride layer, and the relatively high concentration of the alloying element. In addition, the diffusion kinetics of the boride layer had a significant effect on the boron potentials of surface layers produced through different boriding methods. In powder-pack boriding, boron diffusion is affected by the contact surface between the boriding agent and the substrate. In other words, fine particle sizes allow for better diffusion of boron atoms into the material (Ref 27). In the paste-boriding process, the growth kinetics of the boride layer are a function of the thickness of the boron paste on the surface of the material. For instance, as the paste thickness increases, higher boron mobility in the boride layer is observed (at a constant treatment temperature), along with a reduction in the activation energy (Ref 28).

Nevertheless, the optimal boride layer is not necessarily the thickest layer. Thus, the thickness of the boride layer should be matched to the intended application (Ref 30). Using Eq 19 and 20, the diffusion model was extended to estimate the thickness of the Fe_2B and FeB layers formed at the surface of AISI M2 borided steel:

$$l = 2t^{1/2}a_3 D_{Fe_2B}/\{(a_4 + a_3/2)k/[1 - t_0^{Fe_2B}(T)/t]^{1/2} + (a_3/2)k_{FeB}/[1 - t_0^{FeB}(T)/t]^{1/2}\}, \quad \text{m} \qquad \text{(Eq25)}$$

$$u = 2t^{1/2}a_1 D_{FeB}/\left\{(a_4 + a_3/2)k/[1 - t_0^{Fe_2B}(T)/t]^{1/2} + (a_3/2 + a_2 + a_1/2)k_{FeB}/[1 - t_0^{FeB}(T)/t]\right\}, \quad \text{m} \qquad \text{(Eq25)}$$

The behaviors of the parameters $k_{FeB}/[1 - t_0^{FeB}(T)/t]^{1/2}$ and $k/[1 - t_0^{Fe_2B}(T)/t]^{1/2}$ are dependent on the boriding temperature and can be expressed by the following equations, as shown in Fig. 9:

$$\eta(T) = k/[1 - t_0^{Fe_2B}(T)/t]^{1/2} = 1 \times 10^{-33} T^{8.5852}, \quad \text{m s}^{-1/2} \qquad \text{(Eq 27)}$$

$$\varepsilon(T) = k_{FeB}/[1 - t_0^{FeB}(T)/t]^{1/2} = 2 \times 10^{-33} T^{8.3633}, \quad \text{m s}^{-1/2} \qquad \text{(Eq 28)}$$

Thus, Eq 25 and 26 can be modified in the following manner:

$$l = 2t^{1/2}a_3 D_{Fe_2B}/[(a_4 + a_3/2)\eta(T) + (a_3/2)\varepsilon(T)], \quad \text{m} \qquad \text{(Eq 29)}$$

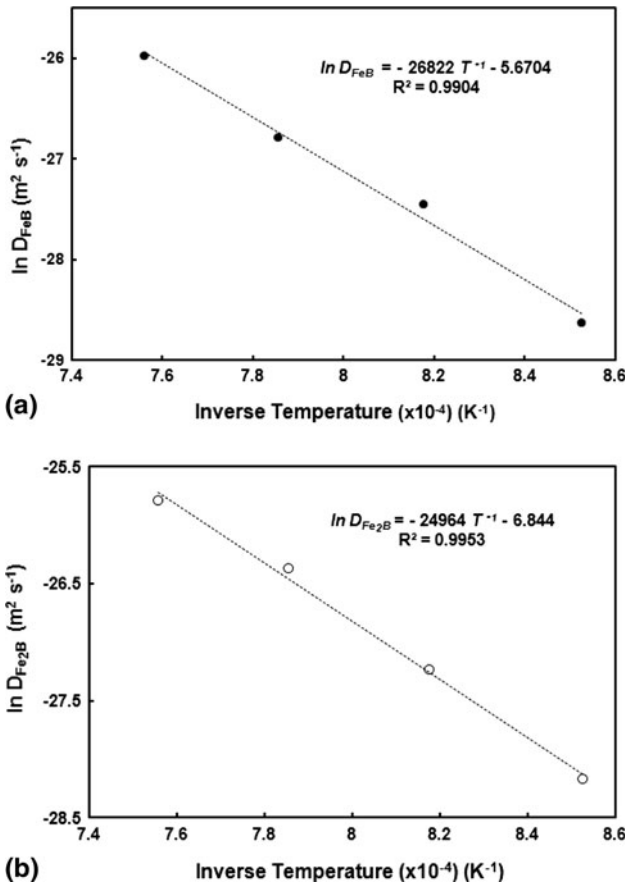

Fig. 8 Dependence between the boron diffusion coefficients and boriding temperature: (a) FeB layer and (b) Fe_2B layer

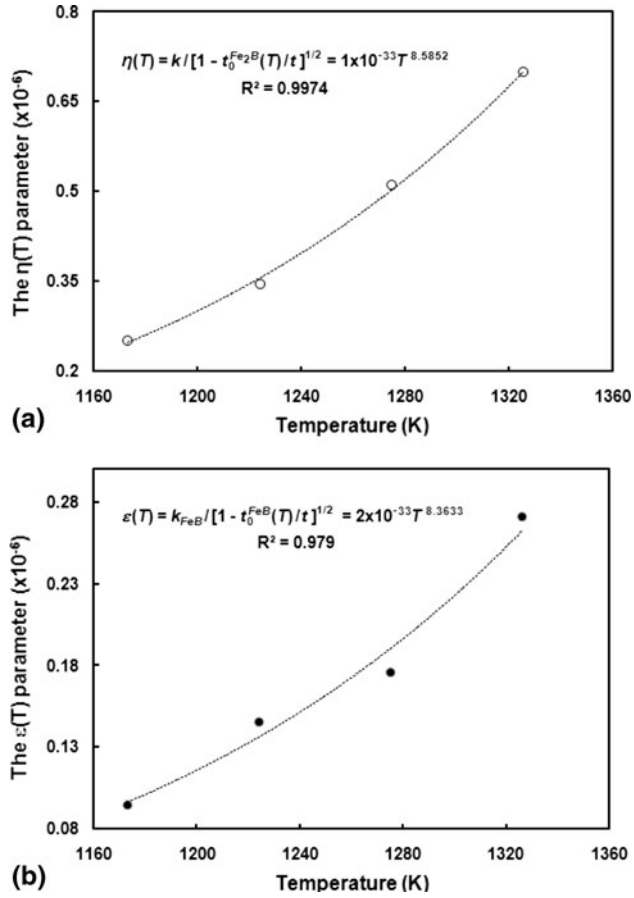

Fig. 9 (a) Behavior of the $\eta(T)$ parameter as a function of temperature and (b) $\varepsilon(T)$ parameter as a function of boriding temperature

Table 1 Activation energy values obtained for different borided steels

Material	Method of boriding	Phases in boride layer	Morphology of the boride layer	Activation energy of FeB layer, kJ mol^{-1}	Activation energy of Fe_2B layer, kJ mol^{-1}	Reference
AISI M2	Paste	FeB, Fe_2B	Smooth	283	239.4	28
AISI H13	Powder pack	FeB, Fe_2B, CrB, Cr_2B	Smooth	…	186.2	29
AISI 316L	Powder pack	FeB, Fe_2B, CrB, Cr_2B, Ni_3B	Smooth	204	198	20
AISI M2	Powder pack	FeB, Fe_2B, CrB, Cr_2B	Smooth	223	207	This study

$$u = 2t^{1/2} a_1 D_{FeB} / [(a_4 + a_3/2)\eta(T) + (a_3/2 + a_2 + a_1/2)\varepsilon(T)], \quad \text{m} \qquad \text{(Eq 30)}$$

Using Eq 29 and 30, the variations in the thicknesses of the Fe_2B and FeB layers as a function of the temperature and exposure time for the powder-pack boriding of AISI M2 steel are represented by contour plots (Fig. 10). In borided high-alloy steels, the optimal thickness of the boride layer is 15-20 μm, which allows the FeB/Fe_2B layers to be applied to tools used for the chipless formation of metals (Ref 30).

Sen et al. (Ref 8) proposed several empirical equations (i.e., Paraboloid, Gaussian, and Lorentzian equations) to determine the thicknesses of the composite boride layers (FeB + Fe_2B) of different borided steels as a function of the exposure time and boriding temperature. In this study, the constant values of the Paraboloid, Gaussian, and Lorentzian equations presented in Tables 2 and 3 were adjusted to the experimental data of boride layers (FeB and Fe_2B) obtained at temperatures of 1173-1323 K and exposure times of 4, 6, and 8 h for the powder-pack boriding of AISI M2 steel.

In addition, the Paraboloid, Gaussian, and Lorentzian equations were used to estimate the thicknesses of the Fe_2B and FeB layers at an exposure time of 10 h and different boriding temperatures (Fig. 11), and the results were compared to those obtained from Eq 29 and 30 for AISI M2 borided steels. The results obtained from Eq 29 and 30 were in good agreement with the experimental data and the theoretical results of the empirical equations shown in Tables 4 and 5. Hence, Eq 29 and 30 can be used as a simple tool to predict the thickness of the FeB and Fe_2B layer on borided steels, according to their practical applications.

5. Conclusions

The growth kinetics of FeB/Fe_2B layers formed at the surface of AISI M2 borided steel were estimated at temperatures of 1123-1323 K and different exposure times. The results revealed that diffusion-controlled growth occurred in both

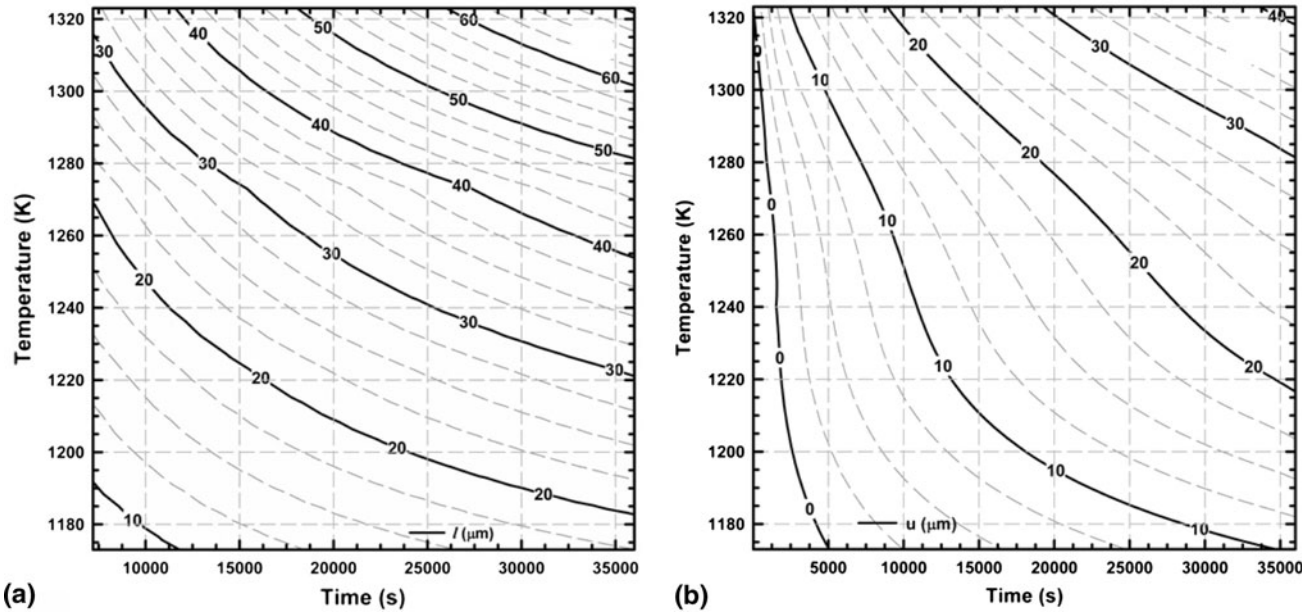

Fig. 10 Contour plots estimated by Eq 29 and 30 that describe the evolution of surface layers obtained by the powder-pack boriding of AISI M2 steel: (a) Fe_2B layer and (b) FeB layer

Table 2 Empirical equations used in the estimation of the Fe_2B layer thickness formed at the surface of AISI M2 steel boriding by the powder-pack method

Equations	Formulas
Paraboloid	$l(t,T) = 1053.817254 + 1.202368 \times 10^{-3} t - 1.940696T - 9.999302 \times 10^{-9} t^2 - 8.834597 \times 10^{-4} T^2 \quad (R^2 = 0.960356)$
Gaussian	$l(t,T) = 518.033219 \exp\left\{-\frac{1}{2}\left[\left(\frac{t - 42512.505551}{28413.326830}\right)^2 + \left(\frac{T - 1823.888569}{251.659694}\right)^2\right]\right\} \quad (R^2 = 0.998574)$
Lorentzian	$l(t,T) = \frac{78.832122}{\left[1 + \left(\frac{t - 37324.695805}{29750.474383}\right)^2\right]\left[1 + \left(\frac{T - 1361.633125}{104.111833}\right)^2\right]} \quad (R^2 = 0.996017)$

t = exposure time, s; T = boriding temperature, K

Table 3 Empirical equations used in the estimation of the FeB layer thickness formed at the surface of AISI M2 steel boriding by the powder-pack method

Equations	Formulas
Paraboloid	$u(t,T) = 215.154790 + 1.343046 \times 10^{-3} t - 0.495677T - 1.750426 \times 10^{-8} t^2 + 2.574646 \times 10^{-4} T^2 \quad (R^2 = 0.942907)$
Gaussian	$u(t,T) = 84.607731 \exp\left\{-\frac{1}{2}\left[\left(\frac{t - 34159.854302}{18705.046854}\right)^2 + \left(\frac{T - 1535.069970}{174.201179}\right)^2\right]\right\} \quad (R^2 = 0.963663)$
Lorentzian	$u(t,T) = \frac{45.223055}{\left[1 + \left(\frac{t - 32346.112903}{19368.700584}\right)^2\right]\left[1 + \left(\frac{T - 1356.470711}{102.338823}\right)^2\right]} \quad (R^2 = 0.940648)$

t = exposure time, s; T = boriding temperature, K

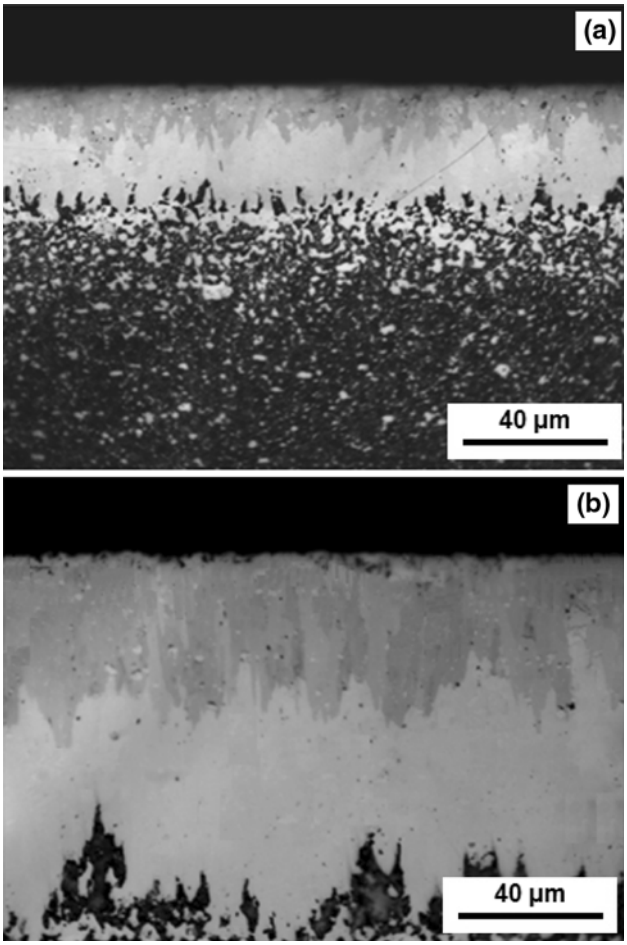

Fig. 11 Cross-sectional views of FeB/Fe_2B layers formed as a consequence of the boriding of AISI M2 steel: (a) 1173 K with 10 h of exposure and (b) 1323 K with 10 h of exposure

boride layers, and the presence of alloying elements in the substrate diminished the kinetics of the layers. The proposed diffusion model was used to estimate the boron diffusion coefficients of the FeB/Fe_2B layers and the thicknesses of the boride layers under the applied set of experimental parameters. In addition, the experimental data obtained at 10 h of exposure and different boriding temperatures were in agreement with the theoretical results of the proposed model and various empirical models presented in the literature.

Table 4 Experimental and predicted values of the Fe_2B layer thicknesses at temperatures of 1173, 1223, 1273, and 1323 K with 10 h of exposure

	Temperature, K			
Equations	**1173**	**1223**	**1273**	**1323**
Predicted Fe_2B layer thicknesses, μm				
Paraboloid	23.28	32.08	45.30	62.94
Gaussian	17.79	29.17	45.96	69.61
Lorentzian	18.37	28.37	45.61	69.15
From Eq 29	17.48	30.50	45.90	70.60
Experimental Fe_2B layer thickness, μm	19.66	32.81	51.83	72.28

Table 5 Experimental and predicted values of the FeB layer thicknesses at temperatures of 1173, 1223, 1273, and 1323 K with 10 h of exposure

	Temperature, K			
Equations	**1173**	**1223**	**1273**	**1323**
Predicted FeB layer thicknesses, μm				
Paraboloid	13.64	19.70	27.05	35.68
Gaussian	9.71	16.92	27.15	40.13
Lorentzian	10.36	16.17	26.22	39.44
From Eq 30	9.07	16.05	27.01	42.51
Experimental FeB layer thickness, μm	10.17	20.98	28.30	40.24

Acknowledgments

This study has been supported by the research grants 150556 from CONACyT and 20120594 from the Instituto Politecnico Nacional in Mexico. The authors wish to thank M. en C. Omar Novelo and Omar Damian Mejia for their valuable collaboration for this study.

References

1. C.M. Brakman, A.W.J. Gommers, and E.J. Mittemeijer, Boriding of Fe and Fe C, Fe-Cr, and Fe-Ni Alloys: Boride Layer Growth Kinetics, *J. Mater. Res.*, 1989, **4**, p 1354–1370
2. J.R. Davis, *Surface Hardening of Steels: Understanding the Basics*, ASM International, Materials Park, OH, 2002
3. S. Sahin, Effects of Boronizing Process on the Surface Roughness and Dimensions of AISI, 1020, AISI, 1040 and AISI, 2714, *J. Mater. Process. Technol.*, 2009, **209**, p 1736–1741

4. J. Pelleg and M. Judelewicz, Diffusion in the B-α-Fe System and Compound Formation Between Electron Gun Deposited Boron Thin Films and Steel Substrate, *Thin Solid Films*, 1992, **215**, p 35–41
5. K. Raic, Z. Acimovic, N. Vidojevic, and N. Novovic-Simovic, Modelling of Fe_2B Boride Layer Growth, *J. Serb. Chem. Soc.*, 1996, **61**, p 181–188
6. E. Meléndez, I. Campos, E. Rocha, and M.A. Barrón, Structural and Strength Characterization of Steels Subjected to Boriding Thermochemical process, *Mater. Sci. Eng. A*, 1997, **234–236**, p 900–903
7. I. Campos, J. Oseguera, U. Figueroa, J.A. García, O. Bautista, and G. Kelemenis, Kinetic Study of Boron Diffusion in the Paste Boriding Process, *Mater. Sci. Eng. A*, 2003, **352**, p 261–265
8. S. Sen, U. Sen, and C. Bindal, An Approach of Kinetic Study of Borided Steels, *Surf. Coat. Technol.*, 2005, **191**, p 274–285
9. L.G. Yu, X.J. Chen, K.A. Khor, and G. Sundararajan, FeB/Fe_2B Phase Transformation During SPS Pack-Boriding: Boride Layer Growth Kinetics, *Acta Mater.*, 2005, **53**, p 2361–2368
10. I. Campos, R. Torres, G. Ramírez, R. Ganem, and J. Martínez, Growth Kinetics of Iron Boride Layers: Dimensional Analysis, *Appl. Surf. Sci.*, 2006, **252**, p 8662–8667
11. M. Keddam, Computer Simulation of Monolayer Growth Kinetics of Fe_2B Phase During the Paste-Boriding Process: Influence of the Paste Thickness, *Appl. Surf. Sci.*, 2006, **253**, p 757–761
12. I. Campos, O. Bautista, G. Ramírez, M. Islas, J. De la Parra, and L. Zúñiga, Effect of Boron Paste Thickness on the Growth Kinetics of Fe_2B Boride Layers During the Boriding Process, *Appl. Surf. Sci.*, 2005, **243**, p 429–436
13. V.I. Dybkov, Growth of Boride Layers on the 13% Cr Steel Surface in a Mixture of Amorphous Boron and KBF_4, *J. Mater. Sci.*, 2007, **42**, p 6614–6627
14. I. Campos-Silva, M. Ortiz-Domínguez, M. Keddam, N. López-Perrusquia, A. Carmona-Vargas, and M. Elias-Espinosa, Kinetics of the Formation of Fe_2B Layers in Gray Cast Iron: Effects of Boron Concentration and Boride Incubation Time, *Appl. Surf. Sci.*, 2009, **255**, p 9290–9295
15. I. Campos-Silva, M. Ortiz-Domínguez, N. López-Perrusquia, A. Meneses-Amador, R. Escobar-Galindo, and J. Martínez-Trinidad, Characterization of AISI, 4140 Borided Steels, *Appl. Surf. Sci.*, 2010, **256**, p 2372–2379
16. I. Campos-Silva, M. Ortiz-Domínguez, H. Cimenoglu, R. Escobar-Galindo, M. Keddam, M. Elias-Espinosa, and N. López-Perrusquia, Diffusion Model for Growth of Fe_2B Layer in Pure Iron, *Surf. Eng.*, 2011, **27**, p 189–195
17. T.B. Massalski, *Binary Alloys Phase Diagrams*, ASM International, Cleveland, OH, 1990
18. T. Van Rompaey, K.C. Hari Kumar, and P. Wollants, Thermodynamic Optimization of the B-Fe System, *J. Alloys Compd.*, 2002, **334**, p 173–181
19. U. Roy, Phase Boundary Motion and Polyphase Diffusion in Binary Metal-Interstitial Systems, *Acta Metall.*, 1968, **16**, p 243–253
20. I. Campos-Silva, M. Ortiz-Domínguez, O. Bravo-Bárcenas, M.A. Doñu-Ruiz, D. Bravo-Bárcenas, C. Tapia-Quintero, and M.Y. Jiménez-Reyes, Formation and Kinetics of FeB/Fe_2B Layers and Diffusion Zone at the Surface of AISI, 316 Borided Steels, *Surf. Coat. Technol.*, 2010, **205**, p 403–412
21. V.I. Dybkov, W. Lengauer, and P. Gas, Formation of Boride Layers at the Fe-25% Cr Alloy-Boron Interface, *J. Mater. Sci.*, 2006, **41**, p 4948–4960
22. K. Matiasovsky, M. Chrenkova-Paucirova, P. Fellner, and M. Makyta, Electrochemical and Thermochemical Boriding in Molten Salts, *Surf. Coat. Technol.*, 1988, **35**, p 133–149
23. C. Badini, C. Gianoglio, and G. Pradelli, The Effect of Carbon, Chromium and Nickel on the Hardness of Borided Layers, *Surf. Coat. Technol.*, 1989, **30**, p 157–170
24. I.S. Dukarevich, M.V. Mozharov, and A.S. Shigarev, Redistribution of Elements in Boride Coatings, *Metallovedenie i Termicheskaya Obrabotka Metallov*, 1973, **2**, p 64–66
25. K. Genel, I. Ozbek, and C. Bindal, Kinetics of Boriding of AISI, W1 Steel, *Mater. Sci. Eng. A*, 2003, **347**, p 311–314
26. A. Galibois, O. Boutenko, and B. Voyzelle, Mécanisme de formation des couches borurées sur les aciers a haut carbone-1 Technique des pates, *Acta Metall.*, 1980, **28**, p 1753–1763
27. A. Graf von Matuschka, *Boronizing*, Carl Hanser Verlag, Munich, Germany, 1980
28. I. Campos, R. Torres, O. Bautista, G. Ramírez, and L. Zuñiga, Effect of Boron Paste Thickness on the Growth Kinetics of Polyphase Boride Coatings During the Boriding Process, *Appl. Surf. Sci.*, 2006, **252**, p 2396–2403
29. K. Genel, Boriding Kinetics of H13 Steel, *Vacuum*, 2006, **80**, p 451–457
30. W. Fichtl, Boronizing and Its Practical Applications, *Mater. Eng.*, 1981, **2**, p 276–286